Toll-like receptor 4 activates the NLRP3 inflammasome pathway and periodontal inflammaging by inhibiting Bmi-1 expression

ZI-YUE QIN[1,2*], XIN GU[3*], YU-LIAN CHEN[1,2], JIA-BAO LIU[3], CHEN-XING HOU[1], SHI-YU LIN[4], NAN-NAN HAO[3], YAN LIANG[5], WU CHEN[1,2] and HAO-YU MENG[3]

[1]Jiangsu Key Laboratory of Oral Diseases, Nanjing Medical University; [2]Department of Periodontology, The Affiliated Hospital of Stomatology, Nanjing Medical University; Departments of [3]Cardiology and [4]Rheumatology, The First Affiliated Hospital of Nanjing Medical University; [5]Department of Clinical Research, Friendship Plastic Surgery Hospital, Nanjing Medical University, Nanjing, Jiangsu 210029, P.R. China

Received June 18, 2020; Accepted October 9, 2020

DOI: 10.3892/ijmm.2020.4787

Abstract. Overproduction of pro-inflammatory cytokines in the aged, which is called inflammaging, leads to the deterioration of periodontitis. Toll-like receptor 4 (TLR4) plays a role in the regulation of cellular senescence, and its expression increases with age. However, there has been limited research into the molecular mechanisms underlying the onset of periodontal inflammaging, and the interplay between TLR4 and inflammaging. In the present study, wild-type and TLR4 gene knockout mice were used to investigate the activation of the TLR4 pathway in mouse periodontitis and the expression of the nucleotide-binding and oligomerization domain-like receptor 3 (NLRP3) inflammasome, an upstream immune checkpoint during the development of inflammaging. Activation of TLR4 in a mouse model of periodontitis enhanced the expression of a senescence-associated secretory phenotype (SASP), which boosted the inflammaging process. Conversely, TLR4 activation downregulated the expression of B cell-specific Moloney murine leukemia virus integration site 1 (Bmi-1) and promoted the priming of NLRP3 inflammasome, both of which are regulators of SASP. Treating gingival fibroblasts with Bmi-1 inhibitor PTC209, it was demonstrated that TLR4 activated the NLRP3 pathway and the inflammaging process by suppressing Bmi-1. In addition, there was a significant reduction in the expression of Bmi-1 expression in the gingiva of patients with periodontitis compared with healthy controls. In conclusion, the present study demonstrated that TLR4 acted by inhibiting Bmi-1 to enhance the NLRP3 pathway and SASP factors. This cascade of reactions may contribute to the senescence of the periodontium.

Correspondence to: Dr Wu Chen, Department of Periodontology, The Affiliated Hospital of Stomatology, Nanjing Medical University, 136 Hanzhong Road, Nanjing, Jiangsu 210029, P.R. China
E-mail: chenwu@njmu.edu.cn

Dr Hao-Yu Meng, Department of Cardiology, The First Affiliated Hospital of Nanjing Medical University, 300 Guangzhou Road, Nanjing, Jiangsu 210029, P.R. China
E-mail: 15805167259@163.com

*Contributed equally

Key words: periodontitis, inflammaging, senescence-associated secretory phenotype, Toll-like receptor 4, B cell-specific Moloney murine leukemia virus integration site 1, nucleotide-binding and oligomerization domain-like receptor 3

Introduction

Inflammaging refers to chronic sterile inflammation that is characterized by cell senescence and aging (1). Periodontitis, a form of inflammaging, is the most common and widespread oral disease that causes tooth mobility and loss (2). The process of periodontitis destroys tooth-supporting connective tissues and alveolar bone (3). Although dysbiotic microbiological burden may play a role in disease development (4), dysregulated immune responses to the microbial insults ultimately destroy the periodontium (5). Equally, inflammaging induced by host cell pathogens plays a crucial role in the deterioration of the immune system (6,7). Senescent cells are characterized by haphazard secretion of inflammatory cytokines, such as interleukin (IL)-1β, IL-6 and tumor necrosis factor-alpha (TNF-α), which is referred to as the senescence-associated secretory phenotype (SASP) (2,8). Therapeutic agents capable of eliminating inflammatory damage, as well as slowing down or reversing the inflammaging process to maintain health in the periodontium, would provide novel avenues for the treatment of periodontitis.

Toll-like receptor 4 (TLR4) is the main receptor for lipopolysaccharides (LPS) present in gram-negative bacteria (9). The TLR4 protein functions as a key regulator of periodontitis by modulating cell signal transduction, apoptosis, and the quality and magnitude of immune responses (10,11). Polymorphisms in the TLR4 gene are associated with increased risk of periodontitis (12). Studies have evaluated the effect of TLR4 in senescence (13-15). Both *in vivo* and *in vitro* studies have shown that increased expression of TLR4 enhances aging (14,15). Additionally, activation of the TLR4-mediated ERK pathway accelerates skin aging by elevating expression

of SASP factors such as IL-6 or IL-8 (16). Senescent fibroblasts have been hypothesized to express high levels of SASP factors, and exhibit higher expression of biologically active TLR4 compared with other cells in diseased periodontal tissues (17,18). However, there is less focus on the fundamental biological mechanisms underlying the roles of TLR4 and senescent gingival fibroblasts in periodontitis.

It has been demonstrated that B cell-specific Moloney murine leukemia virus integration site 1 (Bmi-1) can reduce cell senescence and SASP (19). Bmi-1 plays important roles in regulating cell cycle and senescence via the inhibition of p16/retinoblastoma protein (Rb) and p19/p53 pathways (19,20). The nucleotide-binding and oligomerization domain-like receptor 3 (NLRP3) regulates age-related inflammation and acts as a positive modulator of aging (21,22). Activation of the TLR4 pathway promotes the priming of the NLRP3 inflammasome, which is composed of the receptor protein NLRP3, Caspase-1 and apoptosis-associated speck-like protein containing a CARD domain (ASC) (23,24). The activated NLRP3 assembles at the inflammasome, leading to the activation of Caspase-1 and secretion of IL-1β, which are key factors in periodontal disease (25). Thus, it was hypothesized that the TLR4 signaling pathway affects Bmi-1 and NLRP3 in the pathogenesis of periodontal inflammaging.

The present study aimed to investigate the regulatory effect of TLR4 signaling pathway on inflammaging processes in the periodontium. A ligature-induced periodontitis model in mice was to study whether TLR4 signaling pathway aggravated the inflammaging process in the periodontium via regulation of Bmi-1 expression and the NLRP3 pathway. Additionallly, Bmi-1 protein expression was evaluated in patients with periodontitis compared with periodontally healthy individuals. These results indicated the anti-inflammaging effects of the TLR4/Bmi-1/NLRP3 pathway in periodontitisl thus, targeting the TLR4/Bmi-1/NLRP3 pathway may serve as a novel anti-inflammaging strategy for therapeutic management.

Materials and methods

Animals and treatment schedule. A completely randomized study design was used. A total of 24 wild-type (WT) C57BL/10 and TLR4 knockout (KO) male and female mice (age, 6-8 weeks old; weight, 20.0-22.0 g) were purchased from the Model Animal Research Center of Nanjing University. They were reared in a room with a controlled environment (22-24˚C, 50±5% relative humidity) in 12:12-h dark/light cycles with access to food and water *ad libitum*. All mice were divided randomly into three groups (8 mice/group): The control group that was not subjected to treatment; and the WT and TLR4 KO groups in which a model of periodontitis was induced. To establish a mouse model of periodontitis, mice were anesthetized via an intraperitoneal injection of 4% chloral hydrate (350 mg/kg). Then, the gingival sulcus of left maxillary second molars was ligated with a 9-0 sterile silk for 21 days. All experiments were carried out according to the guidelines of the Experimental Animal Research Institute of Nanjing Medical University. Approval for the study was obtained from the Nanjing Animal Experimental Ethics Committee (permit no. IACUC-1901052).

Subjects and human gingiva samples. A total of 20 volunteers (age, 20-40 years) were recruited at the Affiliated Hospital of Stomatology at Nanjing Medical University from January 2019 to December 2019. The patient group (n=12) was comprised of 6 males and 6 females, while the control group (n=8) consisted of 4 males and 4 females. The program was approved by the Committee on the Ethics of Nanjing Medical University (permit no. PJ2018-050-001) and complied with the Declaration of Helsinki. All volunteers were required to sign an informed consent form prior to enrolment in the study. Before the study, a detailed medical history was obtained using a questionnaire, while clinical examinations were performed to assess the health of the volunteers. Exclusion criteria included: Pregnancy; the use of any antibiotic medicine in the last 3 months; and any systemic disease that could influence the periodontal status. The clinical periodontal measurements taken included the gingival index, probing pocket depth (PD), gingival recession, clinical attachment level (CAL) and the percentage of sites bleeding on probing (BOP). These measurements were performed by a single calibrated investigator. PD and CAL were measured to the nearest mm at six surfaces of all teeth using a straight periodontal probe. Subjects were divided into two groups based on their clinical periodontal measurements: Healthy, the absence of periodontal disease, PD ≤3 mm, and BOP <10%; and periodontitis, PD >3 mm, BOP ≥10% and presence of bone resorption in the radiographic evaluation. Gingival tissue of healthy donors was obtained surgically from the third molars. Gingival tissue of patients with periodontitis was isolated from the inner wall of the periodontal pocket around the affected tooth with PD ≥5 mm and BOP (+) during periodontal surgery.

Cell cultures and treatment. Mice gingiva tissues were extracted from 5-week-old mice after CO_2 inhalation euthanasia (100% CO_2 at a fill rate of 20% volume displaced/min) and cervical dislocation. The tissues were washed with sterile PBS (cat. no. 10010049; Gibco; Thermo Fisher Scientific, Inc.) supplemented with 100 U/l penicillin-streptomycin (cat. no. 15070063; Gibco; Thermo Fisher Scientific, Inc.) three times. These tissues were sectioned into pieces of 1-2 mm^3, placed into a 35-mm culture dish, and incubated with DMEM (cat. no. 11965092; Thermo Fisher Scientific, Inc.) supplemented with 15% FBS (cat. no. 16140071; Gibco; Thermo Fisher Scientific, Inc.) and 100 U/l penicillin-streptomycin. All cells were cultured under a humidified atmosphere of 5% CO_2 at 37˚C and were also used after 3-6 passages to reduce phenotypic drift. The culture medium was changed every 2 days. Human gingival fibroblasts were cultured using human gingival samples from donors during periodontal surgery or extracted from the third molar according to the same protocol as cells isolated from mice gingiva as described previously. During *in vitro* experiments using mouse gingival fibroblasts, the control group was treated with PBS as a control, and the WT and TLR4 KO groups were treated with 100 ng/ml LPS (MedChemExpress LLC) for 24 h at 37˚C; the TLR4 + PTC209 group was treated with 100 ng/ml LPS and 500 nM PTC209 (MedChemExpress LLC) simultaneously for 24 h at 37˚C. The cells were collected for the different assays after treatment. For *in vitro* experiments using human gingival fibroblasts, the healthy group was treated with PBS as a control;

the periodontitis group was treated with 100 ng/ml LPS from *Porphyromonas gingivalis* (*P. gingivalis*; Invitrogen; Thermo Fisher Scientific, Inc.) for 24 h at 37˚C. The cells were collected for the different assays after treatment.

Micro-computed tomography (CT). Mouse maxillae were fixed in 4% paraformaldehyde solution overnight at 4˚C and scanned on a SkyScan1072 scanner (Bruker Corporation) operated at 45 kV and 253 μA with 0.98˚ rotation between frames used at a detection pixel size of 9 μm. The samples were tightly wrapped in plastic to prevent movement and dehydration during scanning. Mimics17 software supplied with the instrument was used to reconstruct three-dimensional images. Multiplanar reconstruction was performed using reconstruction software NRecon (version 1.6.6.0; Bruker Corporation) and CT-analyzer software CTAn (version 1.13.2.1; Bruker Corporation). All images were reoriented so that the cement-enamel junction (CEJ) and the root apex of the maxillary second molar could simultaneously appear in the same micro-CT slice. The distance of CEJ to the alveolar bone crest (CEJ-ABC) was measured to evaluate bone loss around six sites on the ligated side. The alveolar ridge around the maxillary second molar was selected as the trabecular volume of interest and the bone volume to total volume ratio (BV/TV) was assessed in this region.

Preparation of tissue samples and histochemical staining. The excised left maxillae separated from mice after euthanasia were fixed in 4% paraformaldehyde solution overnight at 4˚C, and then decalcified in EDTA glycerol solution for a month on a rotating table at 4˚C. After fixation, 5-μm sections in the mesiodistal plane were cut from each demineralized specimen embedded in paraffin wax. For hematoxylin-eosin staining, the sections were incubated in hematoxylin for 2 min and eosin for 1 min at room temperature after paraformaldehyde fixation. Five random slides per sample were analyzed using a light microscope (magnification, x200) to visualize sections.

Human gingival samples from donors were fixed in 4% paraformaldehyde solution overnight at 4˚C and embedded in paraffin. They were sectioned into slices with a thickness of ~5 μm. Masson's trichrome staining was performed using a Masson Stain kit at room temperature and the duration of Masson staining steps were according to the manufacturer's instructions (cat. no. D026; Nanjing Jiancheng Bioengineering Institute). Five random fields per sample were analyzed using a light microscope (magnification, x200) to visualize sections.

Tartrate-resistant acid phosphatase (TRAP) staining. TRAP staining was conducted using a TRAP Stain kit (cat. no. D023-1-1; Nanjing Jiancheng Bioengineering Institute) according to the manufacturer's instructions. The nuclei were counterstained with methyl green for 5 min at room temperature. Then, TRAP-positive cells were counted in five random fields per sample under a light microscope (magnification, x400). The images were analyzed and quantified using Image-Pro Plus 6 software (Media Cybernetics, Inc.).

Immunohistochemical staining. Maxilla were dissected, and the maxillary second molar and surrounding tissue were retained to perform immunohistochemistry staining with primary antibodies against TNF-α (cat. no. ab6671; Abcam), IL-6 (cat. no. a0286; ABclonal Biotech Co., Ltd.), IL-1β (cat. no. ab9722; Abcam), p16 (cat. no. ab211542; Abcam), p21 (cat. no. ab188224; Abcam), p53 (cat. no. ab131442; Abcam), p19 (cat. no. sc-1665; Santa Cruz Biotechnology, Inc.), NLRP3 (cat. no. 15101s; Cell Signaling Technology, Inc.), ASC (cat. no. ab175449; Abcam) and Caspase-1 (cat. no. 22915-1-AP; ProteinTech Group, Inc.). Briefly, dewaxed and rehydrated paraffin-embedded sections were boiled for antigen retrieval in citrate-EDTA antigen retrieval solution in a steamer for 30 min. Endogenous peroxidase activity was then blocked with methanol: Hydrogen peroxide (1:10) for 10 min at room temperature. After washing with TBS (pH 7.6), the slides were blocked with 10% normal goat serum (Beyotime Institute of Biotechnology) for 1 h at room temperature and then incubated with the primary antibodies overnight at 4˚C. The dilutions of all antibodies were determined were as follows: TNF-α (1:100), IL-6 (1:200), IL-1β (1:100), p16 (1:100), p21 (1:100), p53 (1:100), p19 (1:100), NLRP3 (1:100), ASC (1:100) and Caspase-1 (1:100). Incubation with a secondary antibody (biotinylated goat anti-rabbit or anti-mouse IgG; 1:200; cat. nos. SA00004-2 and SA00004-1; ProteinTech Group, Inc.) for 1 h at room temperature was then performed. After rinsing with TBS for 15 min, sections were incubated with Vectastain Elite ABC reagent for 45 min at 37˚C. Then, sections were developed with 3,3-diaminobenzidine (2.5 mg/ml) and subsequently counterstained with hematoxylin for 1 min at room temperature. The slides were dehydrated, cleared and mounted. Positive cells were counted under a light microscope (magnification, x400) in five random slides per sample. Images were analyzed and quantified by Image-Pro Plus 6 software (26).

Western blot analysis. Western blot analysis was performed using primary antibodies against TNF-α (cat. no. ab6671; Abcam), IL-6 (cat. no. a0286; ABclonal Biotech Co., Ltd.), IL-1β (cat. no. ab9722; Abcam), p16 (cat. no. ab211542; Abcam), p21 (cat. no. ab188224; Abcam), p53 (cat. no. ab131442; Abcam), p19 (cat. no. sc-1665; Santa Cruz Biotechnology, Inc.), NLRP3 (cat. no. 15101s; Cell Signaling Technology, Inc.), ASC (cat. no. ab175449; Abcam), Caspase-1 (cat. no. 22915-1-AP; ProteinTech Group, Inc.) and GAPDH (cat. no. AP0063; Bioworld Technology, Inc.). Cells were lysed in RIPA protein extraction regent (Beyotime Institute of Biotechnology) after washing with PBS three times to extract total proteins. The homogenate was centrifuged at 13,000 x g for 15 min at 4˚C and the supernatant was collected. BCA protein assays (Beyotime Institute of Biotechnology) were performed to determine protein concentrations. For most blots, proteins (~10 μg/lane) were resolved by SDS-PAGE using 8-15% gradient gels and then transferred to PVDF membranes. Membranes were blocked with 5% non-fat milk for 60 min at room temperature and then incubated with the corresponding primary antibodies overnight at 4˚C. The dilutions of antibodies were determined as follows: TNF-α (1:1,000), IL-6 (1:1,000), IL-1β (1:1,000), p16 (1:1,000), p21 (1:1,000), p53 (1:1,000), p19 (1:500), NLRP3 (1:1,000), ASC (1:1,000) and Caspase-1 (1:1,000). After washing, the membrane was incubated with HRP-conjugated goat anti-mouse or anti-rabbit secondary antibodies (1:2,000; cat. nos. SA00001-1 and SA00001-2; ProteinTech Group, Inc.) for 60 min at room temperature. The membrane was washed

three times in TBS with 0.1% Tween-20 (Beyotime Institute of Biotechnology) and then visualized with HRP Substrate Luminol Reagent (EMD Millipore). Quantification and analysis of blots was performed using Image J (version 1.44; National Institutes of Health) (27).

β-galactosidase activity analysis. β-galactosidase activity was evaluated using a FluoReporter lacZ Flow Cytometry kit (cat. no. F-1930; Thermo Fisher Scientific, Inc.) according to standard procedures. Briefly, cells were resuspended at a concentration of 10^7 cells/ml in staining medium and 100 μl was aspirated into a flow cytometer tube. Fluorodeoxyglucose (FDG) loading was initiated by the addition of 100 μl FDG working solution (2 mM), which was prewarmed at 37˚C in the aforementioned flow cytometer tube. Subsequently, 1.8 ml ice-cold staining medium containing 1.5 μM propidium iodide was added into the flow cytometer tube for 1 min to stop the FDG loading. A DxFLEX flow cytometer (Beckman Coulter, Inc.) was set up and calibrated to detect fluorescein, propidium iodide and forward scatter according to the manufacturer's instructions. All cells were analyzed and processed with CytExpert software 1.1 (Beckman Coulter, Inc.).

Immunofluorescent staining. Paraffinized tissue sections were stained with primary antibodies against Bmi-1 (1:100; cat. no. 5856s; Cell Signaling Technology, Inc.) and vimentin (1:100; cat. no. ab8978; Abcam). After fixation and antigen retrieval, 5-μm-thick paraffinized sections were incubated with 10% with 10% normal goat serum (Beyotime) for 1 h at room temperature to block nonspecific binding. The slides were incubated with the primary antibodies overnight, and then with the corresponding secondary antibodies [Alexa Fluor® 594-conjugated goat anti-mouse (1:200; cat. no. ab150120; Abcam) and Alexa Fluor 488-conjugated goat anti-rabbit (1:200; cat. no. ab150077; Abcam)] for 1 h at room temperature. The dilutions of all antibodies were determined according to the manufacturer's instructions. Additionally, cell nuclei were counterstained with DAPI for 5 min at room temperature (cat. no. D9542; Sigma-Aldrich; Merck KGaA) and sealed with mounting medium to prevent fluorescent quenching. The positive cells were counted under a laser confocal microscope. The fluorescent-positive area was quantified using Image-Pro Plus 6 software (26).

Statistical analysis. Data were presented as the mean ± standard deviation (SD) from three separate experiments and Student's t-tests were used to compare data between the two groups. All data were analyzed using GraphPad Prism 6 (version 6.07; GraphPad Software, Inc.). $P<0.05$ was considered to indicate a statistically significant difference.

Results

TLR4 KO relieves the destruction of periodontal soft and hard tissue. To evaluate the effect of TLR4 KO on the pathogenesis of periodontitis, the maxillary second molar was ligated in 8-week-old WT or TLR4 knockout mice for 21 days. Micro-CT was used to detect the extent of alveolar bone destruction and absorption. Compared with the WT group, the TLR4 KO group exhibited reduced bone loss and lesser reduction of the alveolar bone volume (Fig. 1A, B, E and F). HE staining revealed that the depth of the periodontal pocket and attachment loss in the TLR4 KO group were decreased compared with in the WT group (Fig. 1C). Furthermore, the percentage of TRAP-positive osteoclasts in the alveolar bone of TLR4 KO mice was significantly decreased (Fig. 1D and G). Therefore, the results indicated that TLR4 played a role in the progressive destruction of periodontal tissue.

Deletion of TLR4 slows down the onset of cell senescence and SASP in gingiva. To investigate the downstream roles of TLR4 gene KO in suppressing cell senescence and SASP, the expression levels of cell senescence-associated proteins were examined using immunohistochemical staining. Compared with the WT mice, the expression levels of proteins involved in senescence pathways such as p16, p19, p21 and p53 were significantly upregulated in the periodontal soft tissues of TLR4 KO mice (Fig. 2). When stimulated with LPS *in vitro*, mouse gingival fibroblasts exhibited decreased levels of p16, p19, p21 or p53 proteins in the TLR4 KO group compared with the WT group (Fig. 3A and B). Flow cytometry was used to determine the activity of β-galactosidase, a molecular marker of senescent cells, in gingival fzibroblasts. Significantly reduced β-galactosidase activity was observed in the TLR4 KO group compared with the WT group (Fig. 3C and D).

To assess whether TLR4 KO reduces SASP factors in periodontal tissue, the expression levels of SASP-associated proteins such as IL-1β, IL-6 and TNF-α were examined. Compared with the WT group, the levels of IL-1β, IL-6 and TNF-α were significantly reduced in positive periodontium regions in the TLR4 KO mice (Fig. 4A-F). Similarly, the expression levels of IL-1β, IL-6 and TNF-α in gingival fibroblasts were significantly reduced in the TLR4 KO group compared with in the WT group after stimulation with LPS *in vitro* (Fig. 4G and H). The data indicated that TLR4 exacerbated cellular senescence and intensified SASP factors during the loss of alveolar bone.

TLR4 gene KO upregulates Bmi-1 expression and inhibits the NLRP3 pathway in periodontal soft tissue and gingival fibroblasts. Whereas previous data indicates that Bmi-1 regulates SASP in multiple cells via suppression of p16/Rb and p19/p53/p21 signaling pathways (20), Bmi-1 mechanisms in the aging process have not been established. Data from immunohistochemical staining assays revealed that Bmi-1-positive regions in periodontal soft tissue were significantly higher in the TLR4 KO group compared to the WT group (Fig. 5A and E). Furthermore, the expression of Bmi-1 in gingival fibroblasts was increased in the TLR4 KO group compared with the WT group (Fig. 5F and G).

The NLRP3 inflammasome, a commonly studied inflammasome complex, is considered to be a classical upstream regulator of age-related inflammation, which may activate Caspase-1 and IL-1β (28). Immunohistochemical staining was performed to evaluate the expression of NLRP3 and Caspase-1 in gingiva. The results revealed that expression of NLRP3 and Caspase-1 was reduced in the TLR4 KO group compared with the WT group (Fig. 5B, C and E). In addition, the expression of ASC, a crucial adaptor protein for successful inflammasome activation by the NLRPs and AIM2 (23), was found to be significantly reduced in the TLR4 KO group compared with the WT group (Fig. 5D and E). In gingival fibroblasts, the expression levels of NLRP3, Caspase-1 and

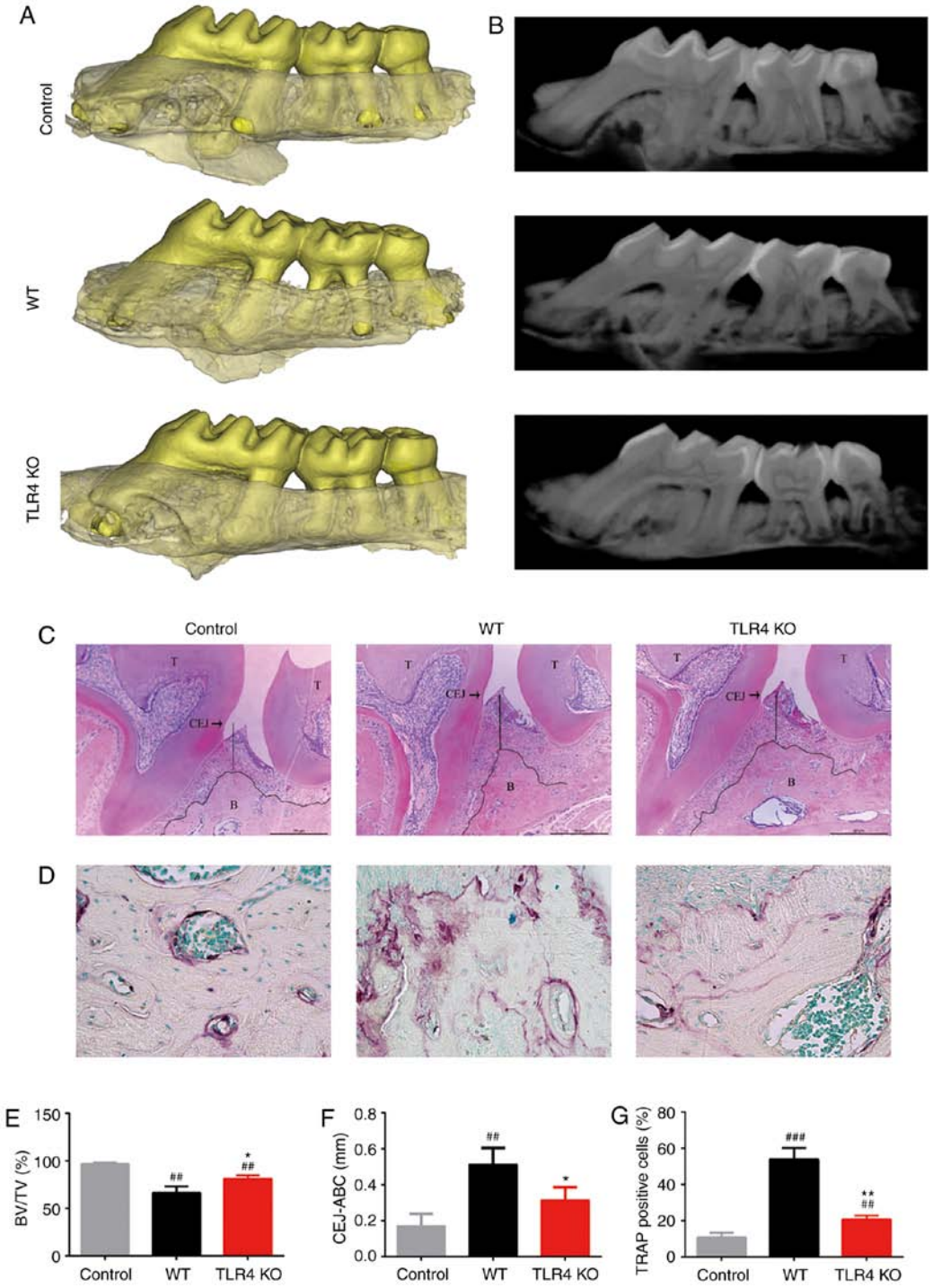

Figure 1. TLR4 KO attenuates the destruction of periodontal tissue in a mouse model of periodontitis. Periodontitis was induced by a 9-0 sterile silk ligature placed inside the gingival sulcus in 8-week-old mice for 21 days. (A) Three-dimensional volume reconstruction images of the left maxilla of mice analyzed by micro-CT scans showed that TLR4 KO could attenuate bone loss in the alveolar ridge. (B) Multiplanar reconstructions on the mesiodistal plane of the left maxilla of mice. The length from buccal to lingual was 500 μm. (C) HE staining showing pathological alterations in mouse periodontium samples derived from different groups (magnification, x100; scale bar, 50 μm). (D) Osteoclasts were visualized by staining for TRAP activity (magnification, x400). (E) Bone volume in the alveolar ridge of the left maxillary second molars was analyzed using the micro-CT scans. (F) Distance between the CEJ and ABC on the distal side of the second maxillary molar was determined using HE-stained frontal sections. (G) Percentage of TRAP-positive cells in the bone surface was calculated. Data are presented as the mean ± SD (n=3/group). $^{\#\#}$P<0.01, $^{\#\#\#}$P<0.001 vs. control; *P<0.05, **P<0.01 vs. TLR4, Toll-like receptor 4; WT, wild-type; KO, knockout; CT, computed tomography; HE, hematoxylin-eosin; TARP, tartrate-resistant acid phosphatase; CEJ, cementum-enamel junction; ABC, alveolar bone crest; BV/TV, bone volume-to-total volume ratio.

ASC were also significantly reduced in the TLR4 KO group (Fig. 5F and G). Therefore, these findings indicated that the Bmi-1 and NLRP3 pathways were involved in TLR4-induced periodontal inflammaging.

Bmi-1 inhibitor PTC209 reverses the suppression of NLRP3 pathway and SASP in TLR4 KO gingival fibroblasts. To further explore the role of Bmi-1, the Bmi-1 inhibitor PTC209 was used to investigate the activation ofNLRP3 pathway and

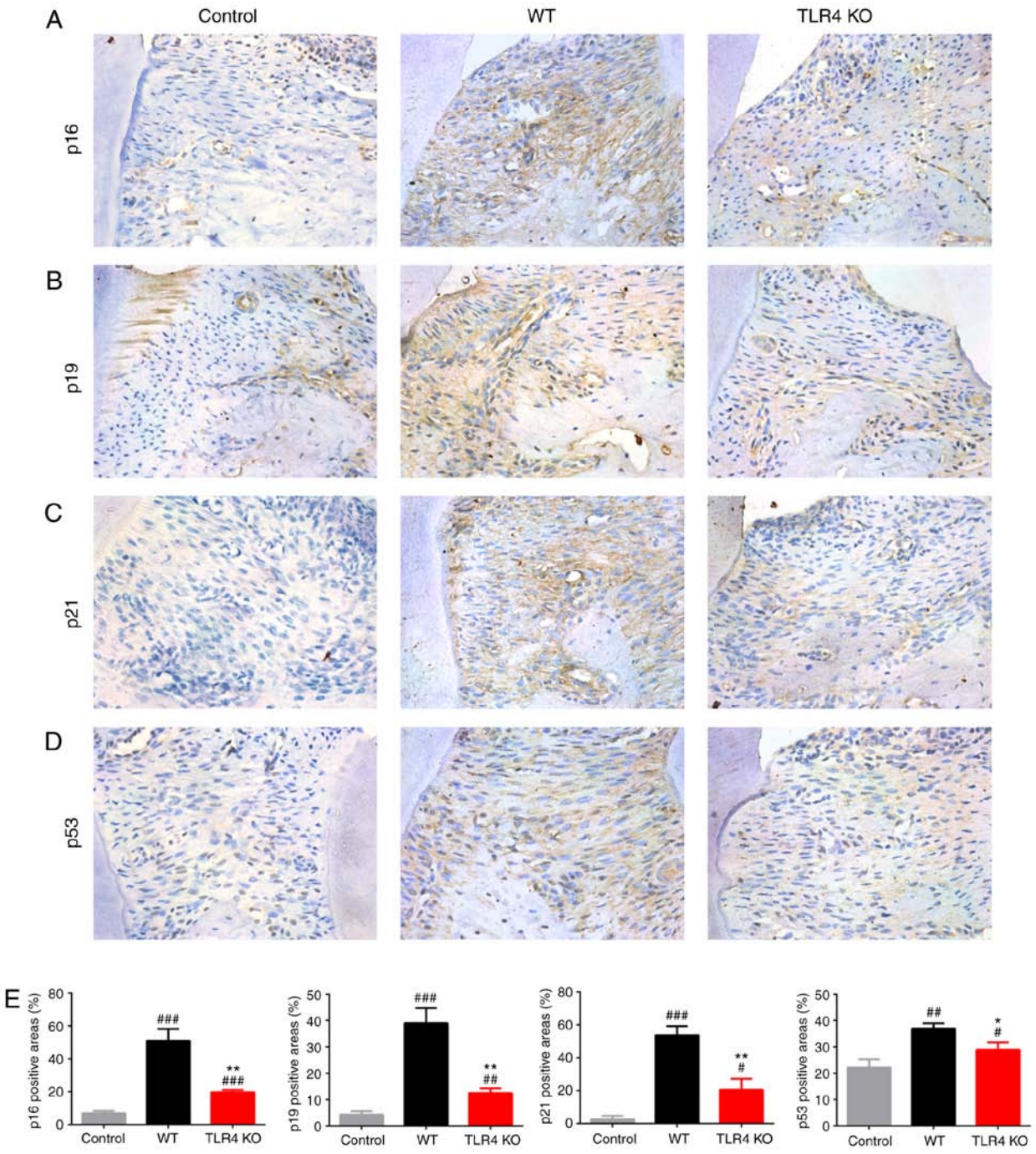

Figure 2. TLR4 KO attenuates senescence in gingiva in a mouse model of periodontitis. Immunohistochemical staining of maxillary paraffin sections was used to evaluate the expression of (A) p16, (B) p19, (C) p21 and (D) p53 (magnification, x400). (E) Histograms showing the percentage of tissue area positive for p16, p19, p21 and p53 in the gingiva. Data are presented as the mean ± SD (n=3/group). $^{\#}$P<0.05, $^{\#\#}$P<0.01, $^{\#\#\#}$P<0.001 vs. control; *P<0.05, **P<0.01 vs. WT. TLR4, Toll-like receptor 4; WT, wild-type; KO, knockout.

the expression of SASP. After stimulating mouse gingival fibroblasts with LPS and 500 nM PTC209 simultaneously for 24 h, downregulation of Bmi-1 was observed in the TLR4 KO + PTC209 group compared with the TLR4 KO group (Fig. 6A and B). Conversely, the expression of NLRP3, Caspase-1 and ASC were increased in the TLR4 KO + PTC209 group compared with the TLR4 KO fibroblasts (Fig. 6A and B). These findings suggested a feedback regulation between Bmi-1 and the NLRP3 pathway.

In addition, the use of PTC209 enhanced the expression of the cell cycle-associated proteins p16, p19, p21 and p53, as well as SASP factors such as IL-1β, IL-6 and TNF-α, in the TLR4 KO group (Fig. 6D, E, G and H). Moreover, the activity of β-galactosidase was increased in the TLR4 KO + PTC209 group compared with the TLR4 KO group (Fig. 6C and F). Together, these data indicated that suppression of Bmi-1 attenuated the anti-inflammaging effect of TLR4 KO in LPS-aged gingival fibroblasts.

Expression of Bmi-1 decreases in the gingival tissues from patients with chronic periodontitis. It was previously observed that there were increased levels of SASP factors such as IL-1β,

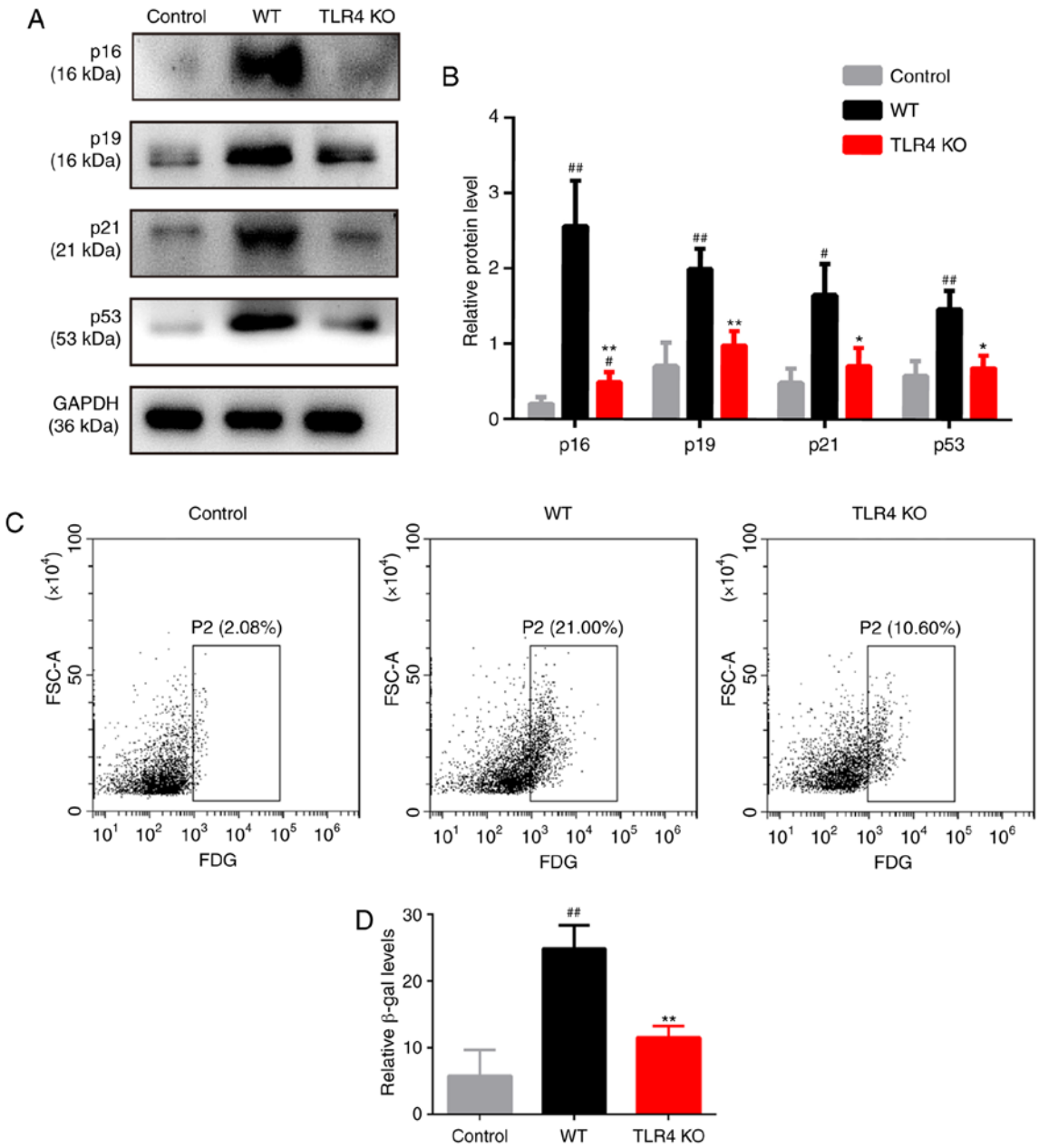

Figure 3. TLR4 KO attenuates senescence in mouse gingival fibroblasts following LPS stimulation. (A) Western blot analysis of p16, p19, p21 and p53 expression in gingival fibroblasts treated with LPS. (B) Relative protein levels of p16, p19, p21 and p53 normalized to GAPDH. (C) β-gal activity was determined via flow cytometry. (D) Relative β-gal levels represented as bar histograms. Data are presented as the mean ± SD (n=3/group). $^{\#}$P<0.05, $^{\#\#}$P<0.01 vs. control; *P<0.05, **P<0.01 vs. WT. TLR4, Toll-like receptor 4; WT, wild-type; KO, knockout; LPS, lipopolysaccharide; β-gal, β-galactosidase; FDG, fluorodeoxyglucose.

IL-6 and TNF-α in the gingival crevicular fluid of patients with periodontal disease (29,30). The findings of the present study suggested that Bmi-1 downregulated SASP factor secretion in mouse periodontitis. Therefore, we compared the expression of Bmi-1 in the gingiva of periodontitis patients and healthy individuals. Masson-trichrome staining showed higher infiltration of inflammatory cells and the destruction of collagen fibers in patients with periodontitis compared with healthy individuals (Fig. 7A). Immunofluorescent assays showed that, compared with the healthy group, the percentage of Bmi-1-positive regions in the gingiva of patients with periodontitis was significantly reduced, particularly in gingival fibroblasts positive for the fibroblast marker vimentin (Fig. 7B and E). Primary human gingival fibroblasts were extracted from subjects in the two groups. Stimulation of the gingival fibroblasts with 100 ng/ml LPS from *P. gingivalis* for 24 h was conducted to imitate an inflammatory microenvironment in periodontitis. Bmi-1 protein expression in gingival fibroblasts was significantly decreased in the periodontitis group compared with the healthy group (Fig. 7C and D). These findings suggested that Bmi-1 was involved in the development of periodontitis.

Discussion

Periodontitis triggered by bacterial infection is a persistent chronic inflammation state of gums and the surrounding structures (3). The innate immune system protects the body from bacterial invasion; however, dysfunction of the immune

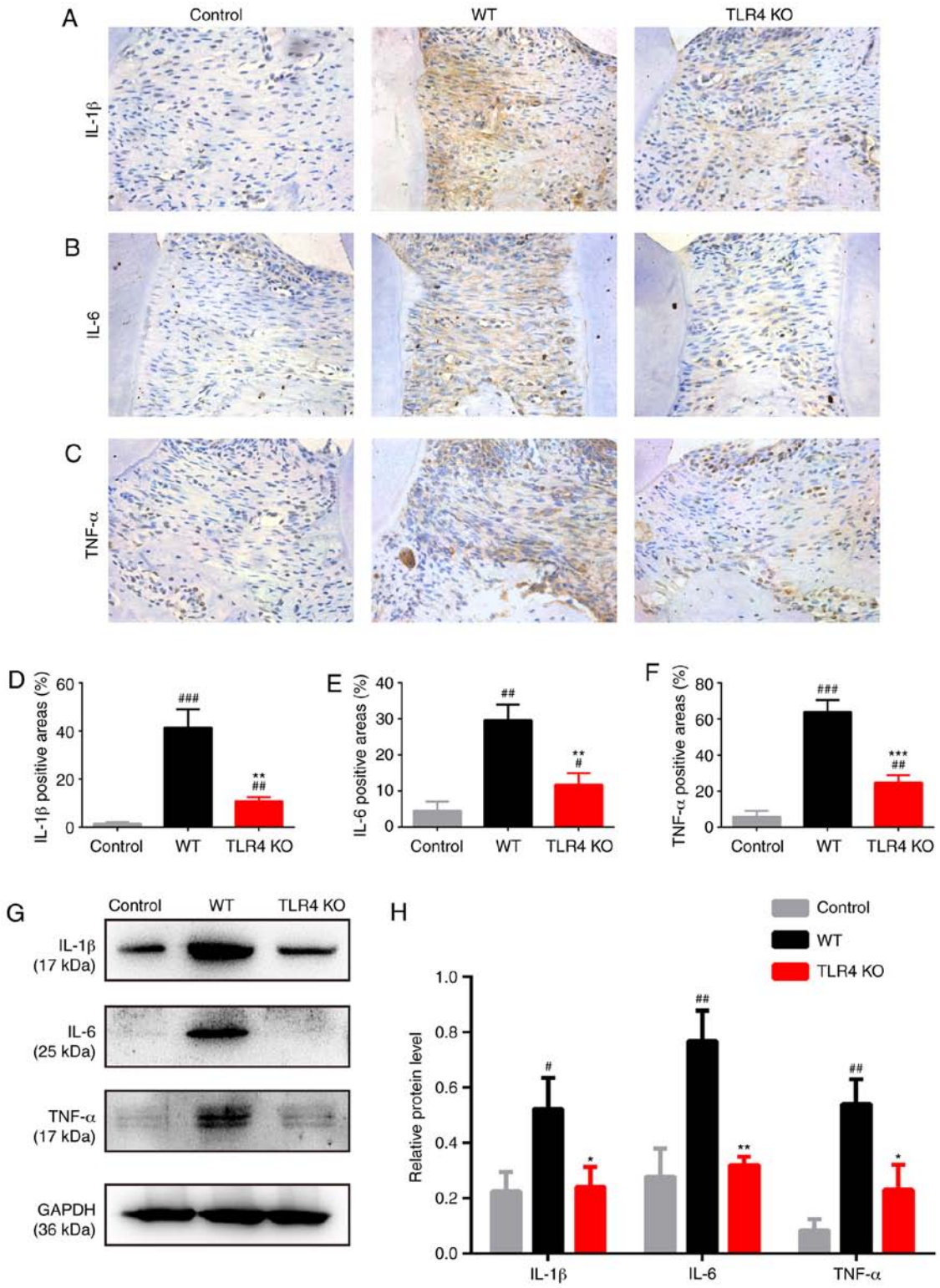

Figure 4. TLR4 KO reduces SASP factor levels in gingival tissues and fibroblasts in a mouse model of periodontitis. Immunohistochemical staining of maxillary paraffin sections was used to evaluate the expression of (A) IL-1β, (B) IL-6 and (C) TNF-α (magnification, x400). Statistical analysis of the percentage of tissue area positive for (D) IL-1β, (E) IL-6 and (F) TNF-α in the gingiva. (G) Western blot analysis of IL-1β, IL-6 and TNF-α expression in gingival fibroblasts following lipopolysaccharide treatment. (H) Relative protein levels of IL-1β, IL-6 and TNF-α normalized to GAPDH. Data are presented as the mean ± SD (n=3/group). $^{\#}$P<0.05, $^{\#\#}$P<0.01, $^{\#\#\#}$P<0.001 vs. control; *P<0.05, **P<0.01, ***P<0.001 vs. WT. TLR4, Toll-like receptor 4; WT, wild-type; KO, knockout; IL, interleukin; TNF, tumor necrosis factor.

system may lead to age-related inflammation (31,32). Previous reports have indicated that age-related inflammation, also referred to as inflammaging, accelerates gingival senescence in gingival tissues (33,34). The persistent presence of senescent cells can foster chronic inflammation and modify the periodontal microenvironment via changes in the levels of SASP factors (34,35). However, the precise mechanism underlying the development of inflammaging in chronic

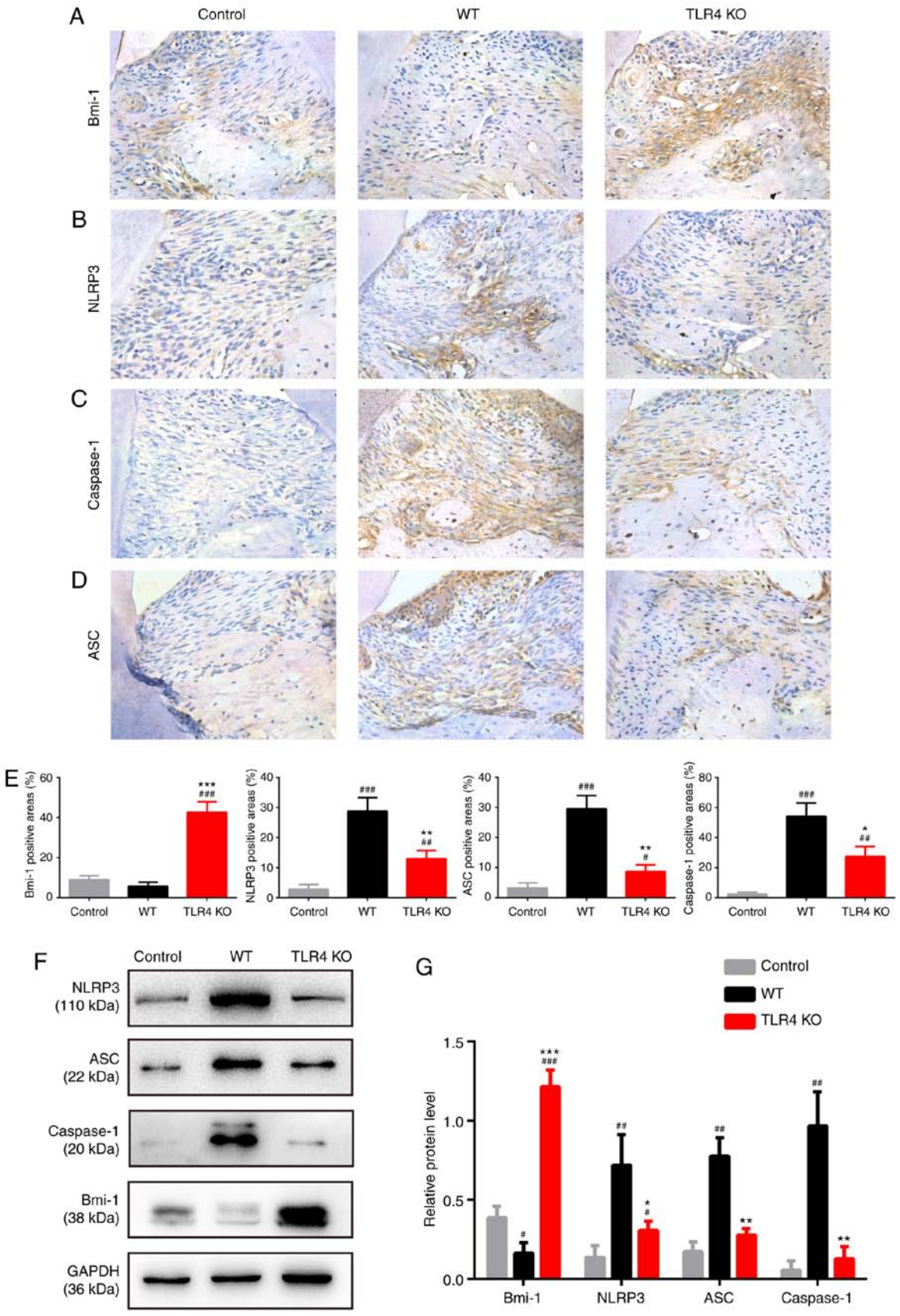

Figure 5. TLR4 KO leads to increased expression of Bmi-1 and suppression of the NLRP3 signaling pathway in gingiva and gingival fibroblasts in a mouse model of periodontitis. Immunohistochemical staining of maxillary paraffinized tissue sections showing the expression of (A) Bmi-1, (B) NLRP3, (C) Caspase-1 and (D) ASC (magnification, x400). (E) Statistical analysis of the percentage of tissue area positive for NLRP3, ASC, Caspase-1 and Bmi-1 in the gingiva. (F) Western blot analysis of NLRP3, ASC, Caspase-1 and Bmi-1 expression in gingival fibroblasts treated with lipopolysaccharide. (G) Relative protein levels of NLRP3, ASC, Caspase-1 and Bmi-1 normalized to GAPDH. Data are presented as the mean ± SD (n=3/group). $^{\#}$P<0.05, $^{\#\#}$P<0.01, $^{\#\#\#}$P<0.001 vs. control; *P<0.05, **P<0.01, ***P<0.001 vs. WT. TLR4, Toll-like receptor 4; WT, wild-type; KO, knockout; Bmi-1, B cell-specific Moloney murine leukemia virus integration site 1; NLRP3, nucleotide-binding and oligomerization domain-like receptor 3; ASC, apoptosis-associated speck-like protein containing a CARD domain.

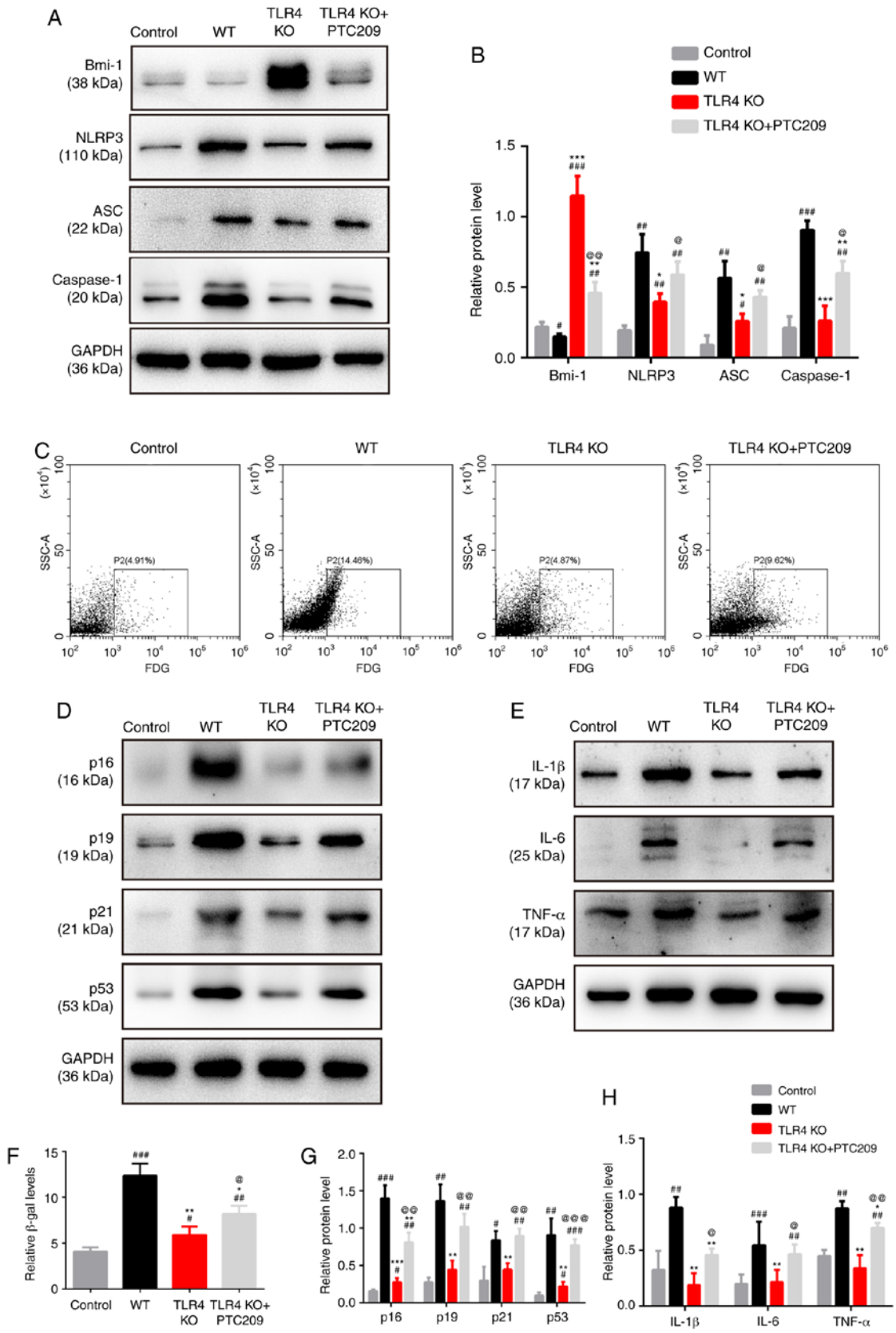

Figure 6. Bmi-1 inhibitor PTC209 attenuates the protective effects of TLR4 KO against senescence and activation of NLRP3 pathway in mouse gingival fibroblasts after LPS stimulation. (A) Western blot analysis of the effect of PTC209 on the expression of Bmi-1, NLRP3, ASC and Caspase-1. (B) Relative protein levels of Bmi-1, NLRP3, ASC and Caspase-1 normalized to GAPDH. (C) Activity of β-gal determined via flow cytometry. (D) Western blot analysis of p16, p19, p21 and p53 protein levels following treatment with PTC209. (E) Western blot analysis of IL-1β, IL-6 and TNF-α protein levels following treatment with PTC209. (F) Histograms showing relative β-gal levels. (G) Relative protein levels of p16, p19, p21 and p53 normalized to GAPDH. (H) Relative protein levels of IL-1β, IL-6 and TNF-α normalized to GAPDH. Data are presented as the mean ± SD (n=3/group). $^{\#}$P<0.05, $^{\#\#}$P<0.01, $^{\#\#\#}$P<0.001 vs. control; *P<0.05, **P<0.01, ***P<0.001 vs. WT; $^{@}$P<0.05, $^{@@}$P<0.01, $^{@@@}$P<0.001 vs. TLR4 KO. TLR4, Toll-like receptor 4; WT, wild-type; KO, knockout; Bmi-1, B cell-specific Moloney murine leukemia virus integration site 1; NLRP3, nucleotide-binding and oligomerization domain-like receptor 3; ASC, apoptosis-associated speck-like protein containing a CARD domain; β-gal, β-galactosidase; IL, interleukin; TNF, tumor necrosis factor; FDG, fluorodeoxyglucose.

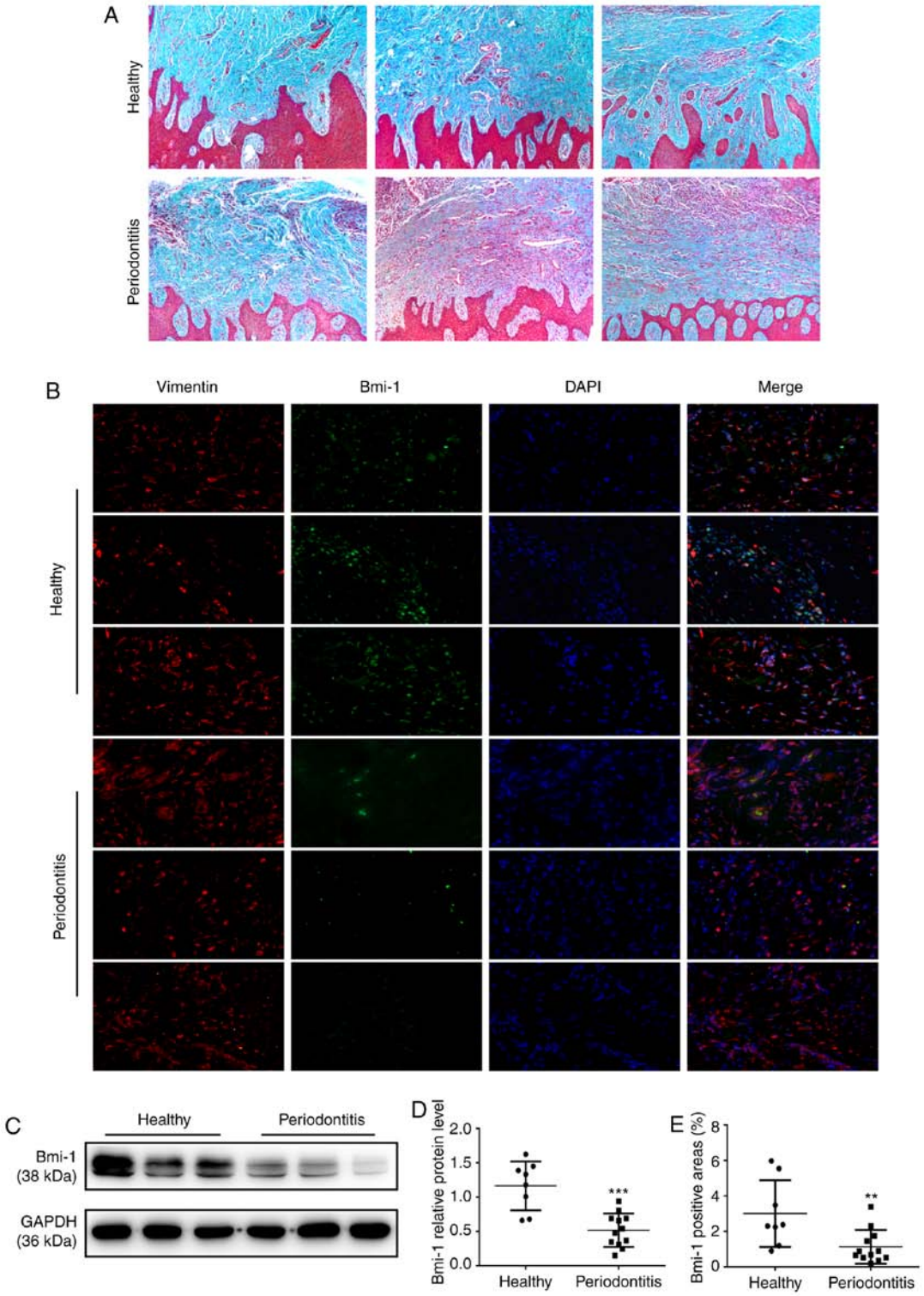

Figure 7. Expression of Bmi-1 is lower in the gingival tissues from patients with chronic periodontitis compared with healthy controls. (A) Pathological alterations of gingival tissues derived from healthy controls and patients with periodontitis as determined by Masson's trichrome assay (magnification, x100). (B) Fluorescence analysis showing the localization of the Bmi-1 and vimentin; the nuclei were stained with DAPI (magnification, x400). (C) Western blot analysis of the expression of Bmi-1 in gingival fibroblasts from different donors. (D) Relative protein levels of Bmi-1 normalized to GAPDH. (E) Bmi-1-positive area shown as a percentage of the tissue area in the gingiva. Data are presented as the mean ± SD. **P<0.01, ***P<0.001 vs. healthy. Bmi-1, B cell-specific Moloney murine leukemia virus integration site 1.

periodontitis has remained largely unclear. The present study indicated that the TLR4 pathway, mobilized by bacterial infection, may suppress Bmi-1 expression and promote activation of the NLRP3 pathway, as well as increasing levels of SASP factors. These events resulted in gingival senescence, which is characterized by excessive secretion of aging biomarkers such as p16, p53 and p21.

LPS, a component of gram-negative bacteria, stimulates inflammation and promotes the resorption of alveolar bone in chronic periodontitis (36). There has been considerable

focus on cellular senescence induced by repeated LPS stimulation (37). It has been reported that bacterial-derived LPS evokes premature alveolar osteocyte senescence and perturbation of SASP factors, promoting the onset of alveolar bone loss (38). The present study observed that LPS stimulated the senescence process and SASP factors in gingival fibroblasts; following LPS stimulation, gingival fibroblasts exhibited a significant increase in the expression of p16, p53 and p21, as well as the secretion of IL-1β, IL-6 and TNF-α. These observations were consistent with a recent study, which showed that LPS increased secretion of IL-6 and TNF-α through p53-dependent activation (39).

TLR4 is a type I integral membrane glycoprotein which can be stimulated by lipopolysaccharide (LPS) (40). The TLR4 pathway affects how innate immune cells sense and respond to infectious stimuli; as a response mechanism, the cells release toxic factors that aggravate periodontitis (41). Results from TLR4 KO mice and gingival fibroblasts demonstrated that TLR4 deletion attenuated the destruction of periodontal tissues by suppressing the expression of senescence-associated proteins and SASP. A previous study found that the activation of the TLR4 pathway regulates the senescence of mouse lung endothelial cells (13). The present study suggested that TLR4 functions as a regulator of cellular senescence in fibroblasts aged in response to LPS stimulation, resulting in persistent chronic low-grade inflammation.

The NLRP3 inflammasome, a commonly studied inflammasome complex, affects patients with chronic periodontitis by catalyzing the initiation and progression of inflammation (42,43). Previous studies suggested that activation of the NLRP3 inflammasome is associated with age-related innate immune activation and may be involved in the onset of periodontitis (21,28). The present study indicated that TLR4 gene KO downregulated the NLRP3 inflammasome and its downstream molecules, ASC and Caspase-1. Whereas other studies have provided evidence that the NLRP3 inflammasome is a key upstream regulator of SASP associated with cellular senescence and inflammatory disease (28,42), the present study suggested that it is TLR4 that regulates the NLRP3 inflammasome and its effector molecules. However, further studies are required to examine whether TLR4 regulates SASP in periodontitis through NLRP3 activation.

It has been reported that Bmi-1 regulates tissue homeostasis and the development of degenerative diseases, and prevents stem cell aging via the Bmi-1/p16 pathway (20,44). There is, however, less data concerning the function of Bmi-1 in the development of periodontitis. The present study showed elevated expression of Bmi-1 in TLR4 KO mice. To further explore the function of Bmi-1 in the pathogenesis of periodontitis, PTC209 was used in TLR4 KO gingival fibroblasts. It was demonstrated that after inhibition of Bmi-1, the reduced activity of the NLRP3 pathway in TLR4 KO fibroblasts and resulting reduction in gingival senescence was attenuated. Thus, Bmi-1 is an important regulator of senescence and inflammation in gingiva, information that could be explored to develop improved therapies for periodontitis.

The present findings suggest that in a mouse model of periodontitis, Bmi-1 negatively regulates TLR4-specific activation of the NLRP3 pathway and SASP secretion in the gingiva. As perturbation of cells in the periodontium contributes to inflammaging in the periodontium (2), the role of Bmi-1 in the development of periodontitis in humans is unknown. The present data indicated that the expression of Bmi-1 in the gingiva was decreased in patients with periodontitis compared with the healthy group, suggesting a close association between Bmi-1 and periodontitis. These results may aid early detection of inflammaging, thus preventing the development of chronic periodontitis. This method may overcome the limitations associated with the evaluation of clinical manifestations of periodontitis or the expression of SASP factors (45). Thus, Bmi-1 may be a reliable predictor of a patient's periodontal status. Longitudinal studies with larger sample sizes are required to validate the hypothesis that Bmi-1 could be a biomarker for periodontitis.

In conclusion, the present study indicated that periodontitis activated the TLR4 pathway in gingival fibroblasts and downregulated Bmi-1. Suppression of Bmi-1 expression accelerated the priming of NLRP3 inflammasome and the accumulation of senescent cells. The increased secretion of age-related inflammatory markers, such as IL-1β, IL-6 and TNF-α, promoted the inflammatory bone destruction in periodontitis. The present study reported an important pathway that potentially mediates the occurrence and development of chronic periodontitis, proposed a novel perspective regarding immune mechanisms involved in periodontitis, and provided a novel future direction for the clinical management of periodontitis.

Acknowledgements

Not applicable.

Funding

This study was supported by grants from the Youth Program of National Natural Science Foundation of China (grant no. 81901416) and the project funded by the Priority Academic Program Development of Jiangsu Higher Education Institutions (grant no. 2018-87).

Availability of data and materials

The datasets used and/or analyzed during the current study are available from the corresponding author on reasonable request.

Authors' contributions

WC and HYM conceived the study and participated in its design, as well as revising and editing the manuscript. ZYQ and XG designed the study, drafted the manuscript and contributed equally to the study. ZYQ, SYL, NNH and YL performed the experiments and collected the data. YLC, CXH and JBL helped collect clinical samples and performed data analysis. All authors had full access to all the data in the study, and take responsibility for the integrity of the data and the accuracy of the data analysis. All authors read and approved the final manuscript.

Ethics approval and consent to participate

All animal experiments were approved by the Nanjing Animal Experimental Ethics Committee (permit no. IACUC-1901052)

and human studies were approved by the Ethical Committee Department, Affiliated Hospital of Stomatology, Nanjing Medical University (permit no. PJ2018-050-001). Written informed consent was obtained from patients or their guardians.

Patient consent for publication

Not applicable.

Competing interests

The authors declare that they have no competing interests.

References

1. Franceschi C, Garagnani P, Parini P, Giuliani C and Santoro A: Inflammaging: A new immune-metabolic viewpoint for age-related diseases. Nat Rev Endocrinol 14: 576-590, 2018.
2. Ebersole JL, Dawson DA III, Emecen Huja P, Pandruvada S, Basu A, Nguyen L, Zhang Y and Gonzalez OA: Age and periodontal health-immunological view. Curr Oral Health Rep 5: 229-241, 2018.
3. Pihlstrom BL, Michalowicz BS and Johnson NW: Periodontal diseases. Lancet 366: 1809-1820, 2005.
4. Mombelli A: Microbial colonization of the periodontal pocket and its significance for periodontal therapy. Periodontol 76: 85-96, 2018.
5. Hajishengallis G: Immunomicrobial pathogenesis of periodontitis: Keystones, pathobionts, and host response. Trends Immunol 35: 3-11, 2014.
6. Franceschi C, Bonafè M, Valensin S, Olivieri F, De Luca M, Ottaviani E and De Benedictis G: Inflamm-aging. An evolutionary perspective on immunosenescence. Ann N Y Acad Sci 908: 244-254, 2000.
7. Kim KA, Jeong JJ, Yoo SY and Kim DH: Gut microbiota lipopolysaccharide accelerates inflamm-aging in mice. BMC Microbiol 16: 9, 2016.
8. Prattichizzo F, De Nigris V, La Sala L, Procopio AD, Olivieri F and Ceriello A: 'Inflammaging' as a Druggable Target: A senescence-associated secretory phenotype-centered view of type 2 diabetes. Oxid Med Cell Longev 2016: 1810327, 2016.
9. Lu YC, Yeh WC and Ohashi PS: LPS/TLR4 signal transduction pathway. Cytokine 42: 145-151, 2008.
10. El-Naseery NI, Mousa HSE, Noreldin AE, El-Far AH and Elewa YHA: Aging-associated immunosenescence via alterations in splenic immune cell populations in rat. Life Sci 241: 117168, 2020.
11. Watanabe K, Iizuka T, Adeleke A, Pham L, Shlimon AE, Yasin M, Horvath P and Unterman TG: Involvement of toll-like receptor 4 in alveolar bone loss and glucose homeostasis in experimental periodontitis. J Periodontal Res 46: 21-30, 2011.
12. Jin SH, Guan XY, Liang WH, Bai GH and Liu JG: TLR4 polymorphism and periodontitis susceptibility: A meta-analysis. Medicine (Baltimore) 95: e4845, 2016.
13. Kim SJ, Shan P, Hwangbo C, Zhang Y, Min JN, Zhang X, Ardito T, Li A, Peng T, Sauler M and Lee PJ: Endothelial toll-like receptor 4 maintains lung integrity via epigenetic suppression of $p16^{INK4a}$. Aging Cell 18: e12914, 2019.
14. Asquith M, Haberthur K, Brown M, Engelmann F, Murphy A, Al-Mahdi Z and Messaoudi I: Age-dependent changes in innate immune phenotype and function in rhesus macaques (Macaca mulatta). Pathobiol Aging Age Relat Dis 2, 2012.
15. Calvo-Rodriguez M, de la Fuente C, Garcia-Durillo M, Garcia-Rodriguez C, Villalobos C and Nunez L: Aging and amyloid β oligomers enhance TLR4 expression, LPS-induced Ca^{2+} responses, and neuron cell death in cultured rat hippocampal neurons. J Neuroinflammation 14: 24, 2017.
16. Seo SW, Park SK, Oh SJ and Shin OS: TLR4-mediated activation of the ERK pathway following UVA irradiation contributes to increased cytokine and MMP expression in senescent human dermal fibroblasts. PLoS One 13: e0202323, 2018.
17. Coppe JP, Patil CK, Rodier F, Sun Y, Muñoz DP, Goldstein J, Nelson PS, Desprez PY and Campisi J: Senescence-associated secretory phenotypes reveal cell-nonautonomous functions of oncogenic RAS and the p53 tumor suppressor. PLoS biology 6: 2853-2868, 2008.
18. Li JP, Chen Y, Ng CH, Fung ML, Xu A, Cheng B, Tsao SW and Leung WK: Differential expression of Toll-like receptor 4 in healthy and diseased human gingiva. J Periodontal Res 49: 845-854, 2014.
19. Lin X, Ojo D, Wei F, Wong N, Gu Y and Tang D: A novel aspect of tumorigenesis-BMI1 functions in regulating DNA damage response. Biomolecules 5: 3396-3415, 2015.
20. Chen H, Chen H, Liang J, Gu X, Zhou J, Xie C, Lv X, Wang R, Li Q, Mao Z, *et al*: TGF-β1/IL-11/MEK/ERK signaling mediates senescence-associated pulmonary fibrosis in a stress-induced premature senescence model of Bmi-1 deficiency. Exp Mol Med 52: 130-151, 2020.
21. Ebersole JL, Kirakodu S, Novak MJ, Exposto CR, Stromberg AJ, Shen S, Orraca L, Gonzalez-Martinez J and Gonzalez OA: Effects of aging in the expression of NOD-like receptors and inflammasome-related genes in oral mucosa. Mol Oral Microbiol 31: 18-32, 2016.
22. Liston A and Masters SL: Homeostasis-altering molecular processes as mechanisms of inflammasome activation. Nat Rev Immunol 17: 208-214, 2017.
23. Schroder K and Tschopp J: The inflammasomes. Cell 140: 821-832, 2010.
24. Qu J, Tao XY, Teng P, Zhang Y, Guo CL, Hu L, Qian YN, Jiang CY and Liu WT: Blocking ATP-sensitive potassium channel alleviates morphine tolerance by inhibiting HSP70-TLR4-NLRP3-mediated neuroinflammation. J Neuroinflammation 14: 228, 2017.
25. Kawahara Y, Kaneko T, Yoshinaga Y, Arita Y, Nakamura K, Koga C, Yoshimura A and Sakagami R: Effects of sulfonylureas on periodontopathic bacteria-induced inflammation. J Dent Res 99: 830-838, 2020.
26. Fathi E and Farahzadi R: Zinc sulphate mediates the stimulation of cell proliferation of rat adipose tissue-derived mesenchymal stem cells under high intensity of EMF exposure. Biol Trace Elem Res 184: 529-535, 2018.
27. Fathi E, Farahzadi R, Valipour B and Sanaat Z: Cytokines secreted from bone marrow derived mesenchymal stem cells promote apoptosis and change cell cycle distribution of K562 cell line as clinical agent in cell transplantation. PLoS One 14: e0215678, 2019.
28. Youm YH, Grant RW, McCabe LR, Albarado DC, Nguyen KY, Ravussin A, Pistell P, Newman S, Carter R, Laque A, *et al*: Canonical Nlrp3 inflammasome links systemic low-grade inflammation to functional decline in aging. Cell Metab 18: 519-532, 2013.
29. Offenbacher S, Barros SP, Singer RE, Moss K, Williams RC and Beck JD: Periodontal disease at the biofilm-gingival interface. J Periodontol 78: 1911-1925, 2007.
30. Romero-Castro NS, Vazquez-Villamar M, Munoz-Valle JF, Reyes-Fernández S, Serna-Radilla VO, García-Arellano S and Castro-Alarcón N: Relationship between TNF-α, MMP-8, and MMP-9 levels in gingival crevicular fluid and the subgingival microbiota in periodontal disease. Odontology 108: 25-33, 2020.
31. Knight ET, Liu J, Seymour GJ, Faggion CM and Cullinan MP: Risk factors that may modify the innate and adaptive immune responses in periodontal diseases. Periodontol 71: 22-51, 2016.
32. Salminen A, Kaarniranta K and Kauppinen A: Immunosenescence: The potential role of myeloid-derived suppressor cells (MDSC) in age-related immune deficiency. Cell Mol Life Sci 76: 1901-1918, 2019.
33. Zhang P, Wang Q, Nie L, Zhu R, Zhou X, Zhao P, Ji N, Liang X, Ding Y, Yuan Q and Wang Q: Hyperglycemia-induced inflamm-aging accelerates gingival senescence via NLRC4 phosphorylation. J Biol Chem 294: 18807-18819, 2019.
34. Wang Q, Zhou X, Zhang P, Zhao P, Nie L, Ji N, Ding Y and Wang Q: 25-Hydroxyvitamin D_3 positively regulates periodontal inflammaging via SOCS3/STAT signaling in diabetic mice. Steroids 156: 108570, 2020.
35. Kuang Y, Hu B, Feng G, Xiang M, Deng Y, Tan M, Li J and Song J: Metformin prevents against oxidative stress-induced senescence in human periodontal ligament cells. Biogerontology 21: 13-27, 2020.
36. Taubman MA, Valverde P, Han X and Kawai T: Immune response: the key to bone resorption in periodontal disease. J Periodontol 76: 2033-2041, 2005.

37. Xia ML, Xie XH, Ding JH, Du RH and Hu G: Astragaloside IV inhibits astrocyte senescence: Implication in Parkinson's disease. J Neuroinflammation 17: 105, 2020.
38. Aquino-Martinez R, Rowsey JL, Fraser DG, Eckhardt BA, Khosla S, Farr JN and Monroe DG: LPS-induced premature osteocyte senescence: Implications in inflammatory alveolar bone loss and periodontal disease pathogenesis. Bone 132: 115220, 2020.
39. Liu J, Zeng J, Wang X, Zheng M and Luan Q: P53 mediates lipopolysaccharide-induced inflammation in human gingival fibroblasts. J Periodontol 89: 1142-1151, 2018.
40. Takeuchi O and Akira S: Pattern recognition receptors and inflammation. Cell 140: 805-820, 2010.
41. Marchesan J, Jiao Y, Schaff RA, Hao J, Morelli T, Kinney JS, Gerow E, Sheridan R, Rodrigues V, Paster BJ, *et al*: TLR4, NOD1 and NOD2 mediate immune recognition of putative newly identified periodontal pathogens. Mol Oral Microbiol 31: 243-258, 2016.
42. Isaza-Guzman DM, Medina-Piedrahita VM, Gutierrez-Henao C and Tobon-Arroyave SI: Salivary Levels of NLRP3 inflammasome-related proteins as potential biomarkers of periodontal clinical status. J Periodontol 88: 1329-1338, 2017.
43. Marchesan JT, Girnary MS, Moss K, Monaghan ET, Egnatz GJ, Jiao Y, Zhang S, Beck J and Swanson KV: Role of inflammasomes in the pathogenesis of periodontal disease and therapeutics. Periodontol 82: 93-114, 2020.
44. Chen G, Zhang Y, Yu S, Sun W and Miao D: Bmi1 overexpression in mesenchymal stem cells exerts antiaging and antiosteoporosis effects by inactivating p16/p19 signaling and inhibiting oxidative stress. Stem Cells 37: 1200-1211, 2019.
45. Kinney JS, Morelli T, Oh M, Braun TM, Ramseier CA, Sugai JV and Giannobile WV: Crevicular fluid biomarkers and periodontal disease progression. J Clin Periodontol 41: 113-120, 2014.